NOVEL LEFT-HANDED TRANSMISSION LINES BASED ON GROUNDED SPIRALS

B. Jokanović[1], and V. Crnojević-Bengin[2]

[1] Institute Imtel, Belgrade, Serbia

[2] Dept. of Electronics, Faculty of Technical Sciences, University of Novi Sad, Serbia,

ABSTRACT: *Novel super-compact ($\lambda_g/13$ by $\lambda_g/13$) left-handed (LH) unit cell ForeS, based on grounded spirals, is analyzed in detail. ForeS exhibits low insertion losses and a large design flexibility: small changes of its inner dimensions, result in resonant frequency tuning range approximately equal to 67%. In the same time, the second harmonic is positioned at more then four times the first resonant frequency. By placing the diodes at the relevant positions, ForeS can be made electronically reconfigurable: 27% resonant frequency tuning range can be achieved, as well as different in- and out-of-band performances. Two LH transmission lines are designed using ForeS that offer a trade-off between LH bandwidth and pass band ripple.*

Key Words: *Left-Handed Metamaterials; Transmission Line Approach; Bandpass Filters.*

1. INTRODUCTION

Although theoretically predicted by Veselago in the late sixties, [1], the existence of LH metamaterials was not experimentally proved until 2000, [2]. From that time, the number of scientific results devoted

to the synthesis of LH media in one, [3]-[6], two, [7], [8], and three dimensions, [9], and its application has dramatically increased.

Metamaterials are artificial structures composed of a number of unit cells with sub-wavelength dimensions, that demonstrate exotic electromagnetic properties usually not found in nature, i.e. arbitrarily small, large, or even negative values of the effective permittivity and permeability. Double-negative or left-handed (LH) metamaterials are those that simultaneously exhibit negative values of effective permittivity and permeability in a certain frequency range. Due to the small electrical size of the unit cells, metamaterials offer a great solution to the design of miniaturized microwave devices. Since nowadays many microwave circuits and devices are designed in planar technology, the synthesis of high-performance compact one-dimensional planar LH metamaterials, i.e. LH transmission lines is of great interest.

In the realization of one-dimensional planar LH metamaterials, two main approaches are widely accepted in the microwave community: (i) resonant-type LH metamaterial design based on unit cells such as split-ring resonators, [6], [10], and (ii) non-resonant transmission line (TL) approach, [11], [12], based on the dual transmission line concept. While the first approach results in narrow-banded LH structures, the second one provides a useful tool for the design of simultaneously low loss and broad bandwidth devices.

The TL approach was almost simultaneously proposed by Oliner, [3] Caloz and Itoh, [4] and Grbic and Eleftheriades, [5]. A dual transmission line is one-dimensional propagating medium that can be described by an equivalent circuit that is the dual of the circuit that models a conventional transmission line. In the dual case, the capacitors are connected in series, while the inductors are placed in a shunt configuration. If the unit cells are sufficiently small (much smaller then the propagating signal

wavelength), such structure can be regarded homogenous, i.e. effective permittivity and permeability can be calculated. It has been shown that the dual transmission lines exhibit negative effective permittivity and permeability in a certain frequency range and, therefore, behave as LH transmission lines.

In this paper, two novel LH transmission lines are proposed, based on a super-compact LH unit cell called ForeS, recently reported in [13]. Firstly, the unit cell ForeS and its modifications are analyzed in detail and the potential of ForeS for application in electronically reconfigurable circuits is investigated. Then, two novel LH TL designs are shown, with different coupling mechanisms between the unit cells. The performances of the lines are determined through simulation and measurements and the LH nature of the proposed lines is verified.

2. CONFIGURATION OF THE UNIT CELL

Unit cell ForeS is based on a ring resonator loaded with four grounded spirals, both mutually coupled and end-coupled to the host microstrip line, as shown in Figure 1. ForeS is realized on 1.575mm Rogers 5880 substrate with $\varepsilon_r = 2.17$, and $tg\delta = 0.0009$, and its overall dimensions are equal to $\lambda_g/13$ by $\lambda_g/13$, where λ_g denotes the guided wavelength in a microstrip line. Relevant dimensions of ForeS are also indicated in Figure 1.

In order to investigate the flexibility of ForeS design, dimensions of the spirals were varied, while the overall dimensions (length L_c, and width W_c) and coupling to the microstrip (gap g_{EC}) remained unchanged, i.e. L_c=9mm, W_c=9mm, and g_{EC} =100μm. Simulations were performed using IE3D Power

Pack Version 10.0 with conductor losses included through σ = 58 MS/m. The obtained results are shown in Table 1 and compared in Figure 2.

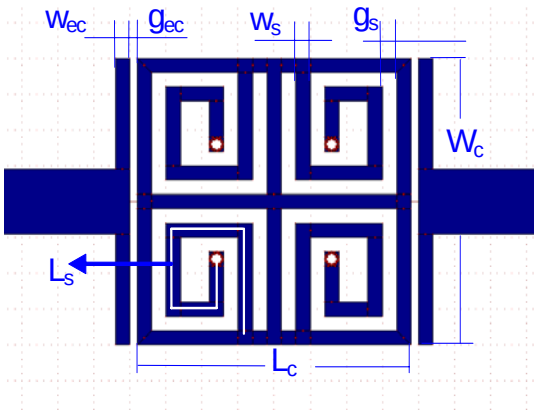

Figure 1 ForeS unit cell with relevant dimensions

TABLE 1 Simulation results for four different ForeSs that occupy the same area

Unit Cell:	ForeS_1	ForeS_2	ForeS_3	ForeS_4
W_S, mm	0.4	0.5	0.6	0.2
g_S, mm	0.1	0.1	0.2	0.1
L_S, mm	28.8	23.05	15.2	54.2
f_R, GHz	1.876	2.35	3.175	1.038
s^1_{21}, dB	-1.86	-1.8	-2.05	-2.7
s^1_{11}, dB	-14.17	-14.5	-13.79	-11.47
B, MHz	95.5	147.67	290	31.95
Q_L	19.64	15.91	10.95	32.49
Q_U	56.39	46.90	29.10	70.17
f_{R2}, GHz	7.75	7 / 8.15	7.9	3.1
s^2_{21}, dB	-1.12	-2 / -1.43	-1.3	-14

To foster the coupling, the gap between the resonator and the microstrip line is kept minimum in all configurations, i.e. g_{EC}=100μm. In this way, low insertion loss at the resonance and good reflection are

insured. Although typically LH structures suffer from high insertion losses, low insertion loss is a specific feature of ForeS, as evident from the results presented in Table 1. Another advantage of ForeS is its large design flexibility: by introducing small changes to the inner dimensions of ForeS, namely by changing W_S and g_S while keeping the overall dimensions fixed, significantly different resonant frequencies can be obtained, ranging from 1.038GHz to 3.18GHz, i.e. 67% different in respect to the highest frequency.

The simulation results reveal that an optimal value for the width of the spiral line, W_S, exists, equal to 400μm. If W_S is reduced below this value (as in the case of ForeS_4), additional insertion loss in encountered, although the lowest resonant frequency is obtained. The simulations also show that the spacing between adjacent spiral turns, g_S, should be kept minimal achievable in standard PCB technology, i.e. equal to 100μm. It can be concluded that the configuration denoted as ForeS_1 offers the best trade-off between the Q-factor, insertion loss and resonant frequency. Furthermore, ForeS_1 is also superior when out-of-band performance is considered. It exhibits the widest stop-band with the highest attenuation level, as can be seen from Figure 2.

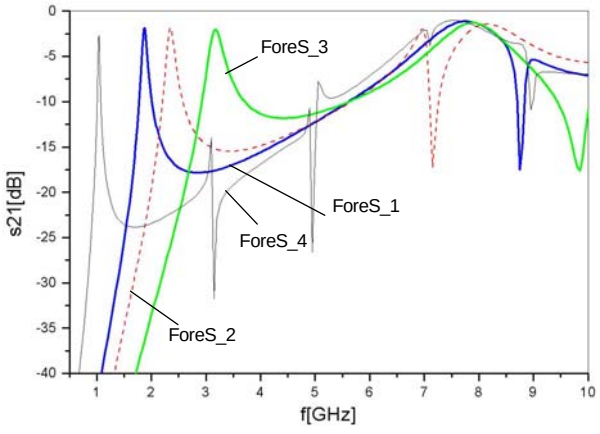

Figure 2 Simulated transmission coefficients for four different ForeSs that occupy the same area

By comparing the responses in Figure 2, it can be noted that the variation of spiral width and gap only influences the first resonance, while the second one remains almost unchanged, around 8.0GHz. In order to fully understand the behavior of ForeS, it is compared with a conventional ring resonator and its modifications, shown in Figure 3, that have the same overall dimensions and the gap to the host microstrip. The simulated responses of all structures depicted in Figure 3 are shown in Figure 4 for the lossy case.

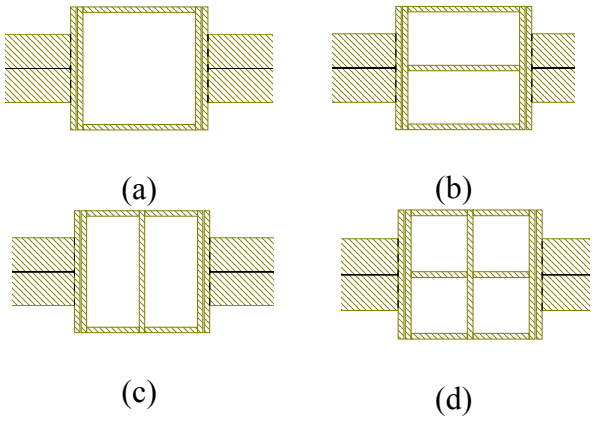

Figure 3 (a) Conventional ring resonator and its modifications used for comparison: (b) with horizontal line, (c) with vertical line, (d) with both lines

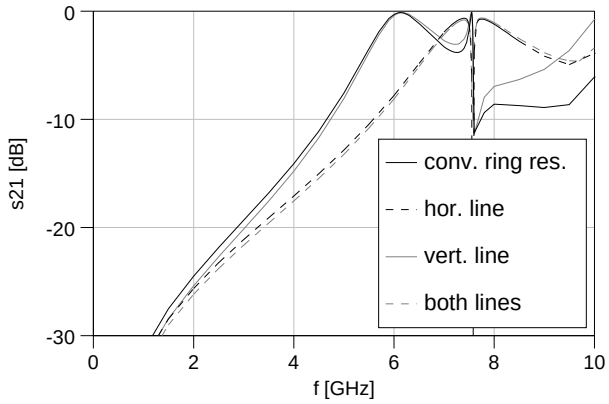

Figure 4 Simulated transmission coefficients of a conventional ring resonator and its modifications shown in Figure 3

It can be seen that the ring resonator alone is responsible for the existence of the second harmonic of ForeS, positioned around 8GHz. This peak is shifted towards higher frequencies due to the existence of the horizontal line in the ring resonator. Vertical line, however, has no influence on the performances and could be removed from the original ForeS design. Additional simulations of ForeS without the vertical line were performed that support this conclusion.

In Figure 5 and Table 2, the influence of the number of spiral turns, N_s, to performances of ForeS_1 is analyzed. As the number of turns increases, the resonant frequency significantly decreases, due to the increased inductance of the spirals. In the same time, insertion loss increases, and the unloaded Q-factor decreases. These results also illustrate high design flexibility of the ForeS: small changes in the geometry significantly influence its performances. Since the miniaturization is the most relevant issue in the design of LH transmission lines presented in this paper, ForeS_1 with the highest achievable number of turns, i.e. N_s=3.25, will be used.

TABLE 2 Simulation results for ForeS_1 with different number of spiral turns, N_s

N_s	0.25	0.5	0.75	1.25	3.25
f_R, GHz	4.35	4.06	3.5	2.59	1.876
s^I_{21}, dB	-0.27	-0.616	-0.864	-1.09	-1.86
B, MHz	600	400	280	160	95.5
Q_L	7.25	10.15	12.5	16.19	19.64
Q_U	120.28	76.75	69.29	72.94	56.39

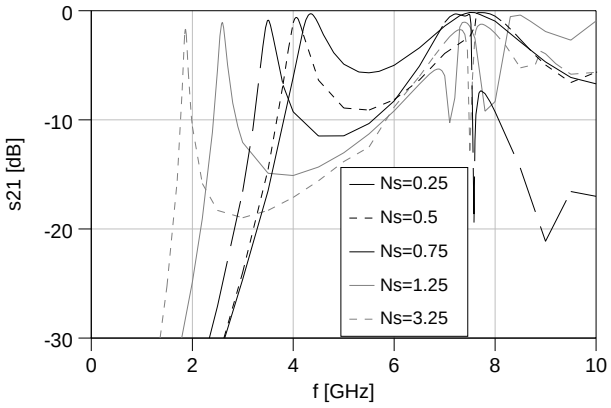

Figure 5 Comparison of simulated transmission coefficients for ForeS_1 with different number of spiral turns, N_s

3. RECONFIGURABILITY OF THE UNIT CELL

Apart from the large design flexibility of the ForeS, discussed in the previous section and related to the change of its inner dimensions, the ForeS also exhibits great potential for electronic reconfigurability. By placing the diodes at relevant positions, represented with light square patches in Figure 6, and by applying bias voltage, various modifications of ForeS can be generated. Different types of diodes can be used to reconfigure the ForeS: PIN diodes, varactor or Schottky barrier diodes. Diodes in each pair should be oppositely oriented: left and right in respect to the central biasing line, so beam lead anti-parallel diode pairs or common cathode diode arrangement can be used.

By switching the bias voltage on or off, various modifications of ForeS can be generated, shown in Figure 7. All four configurations have been simulated using metal patches instead of diodes and the results obtained are summarized in Table 3. Physical dimensions in all cases are the same as for ForeS_1 (given in Table 1).

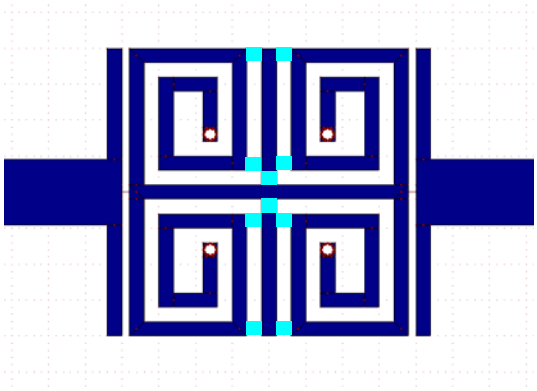

Figure 6 ForeS unit cell with positions at which diodes can be placed, indicated with light patches

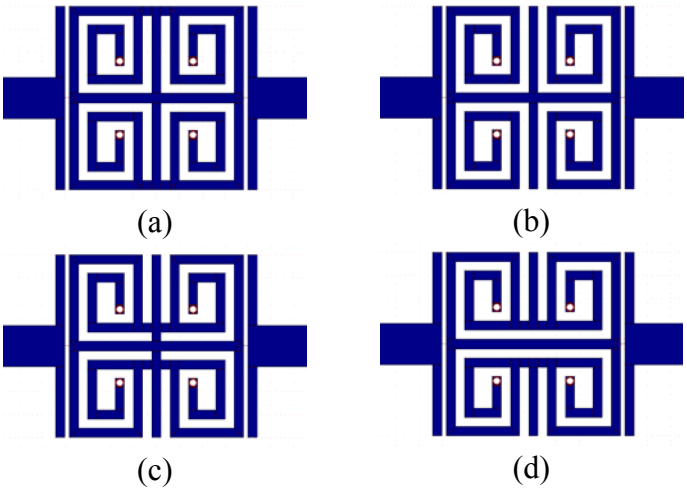

Figure 7 Different configurations obtained by means of electronic reconfigurability:

(a) original ForeS (End-Connected Cross), (b) End-Opened Cross,

(c) Center-Connected Cross, (d) Center-Disconnected Cross

It can be seen that by applying bias voltage at the relevant positions, significantly different resonant frequencies can be obtained. In this way, the tuning range approximately equal to 27% is achieved.

The configuration End-Opened Cross exhibits the lowest resonant frequency, but has the disadvantage of the second resonance positioned as low as 3.7 GHz. Center-Disconnected Cross shows very good characteristics: low resonant frequency, low insertion loss at resonance, small reflection, and high Q-factor, while the second harmonic appears at 6.0 GHz. The best out-of-band response is exhibited by the original ForeS, with the second harmonic shifted to 7.75 GHz.

TABLE 3 Simulation results for ForeS and its modifications

Unit Cell:	ForeS	End-Open.	Cent.-Conn.	Cent.-Disconn.
f_{R1}, GHz	1.876	1.53	2.0	1.59
$s^1_{21,}$ dB	-1.86	-1.726	-1.87	-1.58
$s^1_{11,}$ dB	-14.17	-14.85	-14.3	-15.75
B, MHz	95.5	58.5	108.3	69
Q_L	19.64	26.15	18.47	23.04
Q_U	56.39	79.75	52.78	75.56
f_{R2}, GHz	7.75	3.72	6.0	6
$s^2_{21,}$ dB	-1.12	-1.428	1.22	-1.17
f_{R3}, GHz	-	6.0	6.8	6.775
$s^3_{21,}$ dB	-	-1.652	-1.02	-1.0

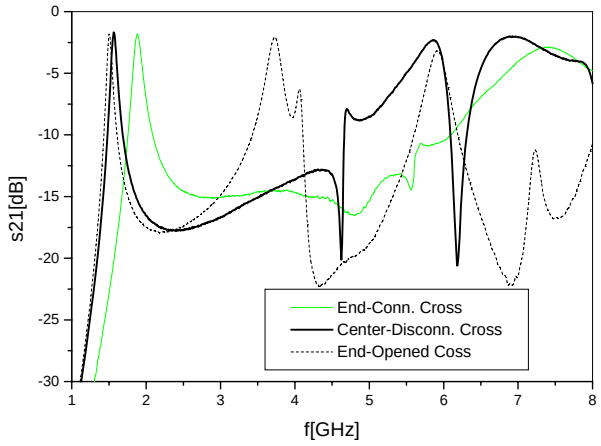

Figure 8 Measured transmission coefficients of different configurations obtained by means of electronic reconfigurability

Three configurations that offer the best performances have been fabricated using the standard PCB technology. The measured responses are compared in Figure 8. Very good agreement with simulations has been achieved, thus validating the simulation results.

4. LH TRANSMISSION LINE DESIGN

4.1. LH Transmission Line with Direct Coupling

By cascading the unit cells ForeS, novel LH transmission lines with direct coupling can be designed. In this case, the adjacent ForeSs are placed at 100 μm distances and directly coupled one to the other. Two lines of this type have been fabricated using the standard PCB technology, with N=2 and N=3 unit cells. The photographs of the fabricated lines are shown in Figure 9.

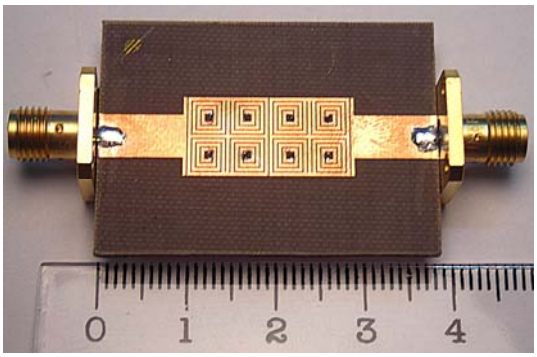

(a)

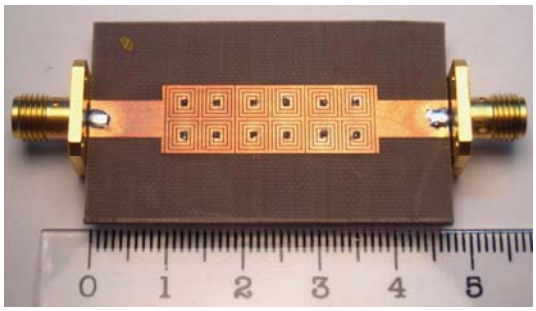

(b)

Figure 9 Fabricated LH transmission lines with direct coupling of adjacent ForeSs:

(a) N=2 unit cells and (b) N=3 unit cells

Left-handedness of the proposed structure is evident from the comparison of the measured phases of transmission coefficients obtained from two lines with different numbers of unit cells, *N*=2 and *N*=3. In Figure 10 unwrapped phase is shown. Unwrapping has been performed in respect to the left edge of the pass band. It can be seen that a phase advance exists in the pass band, thus demonstrating backward propagation.

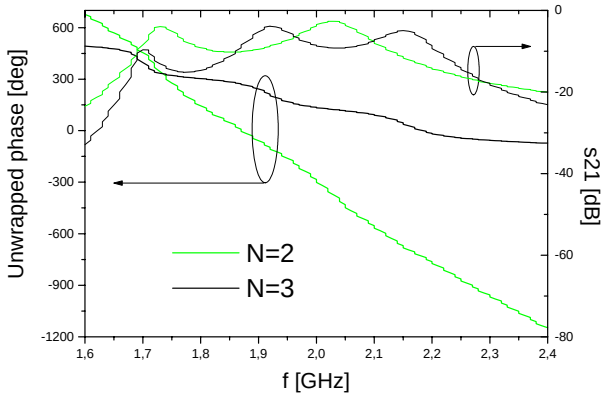

Figure 10 Measured transmission coefficients and unwrapped phase responses of two LH transmission lines with *N*=2 and *N*=3 unit cells

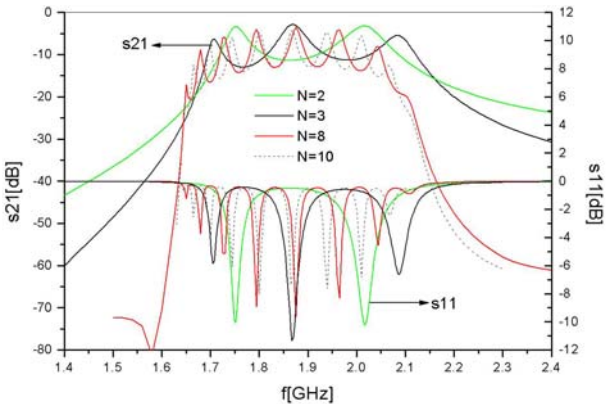

Figure 11 Simulated transmission and reflection coefficients of the proposed LH transmission line with the direct coupling, for different number of the unit cells, *N*

In Figure 11, the influence of the number of unit cells, *N*, to performances of the proposed line is analyzed. It can be seen that, as the number of the unit cells is increased, the steeper response is obtained, while the insertion loss and fractional bandwidth do not change significantly.

To verify the simulation results, LH lines with *N*=2 and *N*=3 unit cells were fabricated. The measured responses are shown in Figure 12.

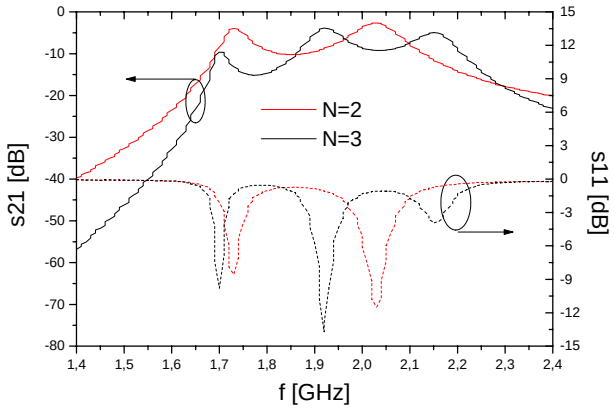

Figure 12 Measured transmission and reflection coefficients of the proposed LH transmission line with the direct coupling, for different number of the unit cells, *N*

A good agreement between the simulated and the measured responses can be observed. It can be seen that, although exhibiting fractional LH bandwidth approximately equal to 30%, the proposed LH transmission lines generally suffer from high ripple in the pass band.

4.2. LH Transmission Line with Weakly Coupled Unit Cells

In order to reduce the pass band ripple that exists in the case of LH transmission lines with the direct coupling, novel configuration is proposed, where additional vertical lines are placed between the

adjacent ForeSs. The width of these lines is equal to 400 μm. In Figure 13, photographs of the prototypes with *N*=2 and *N*=3 unit cells are shown.

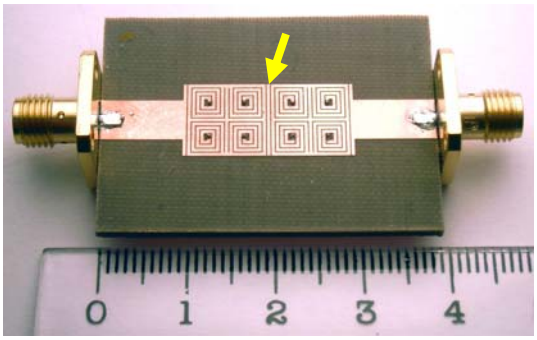

(a)

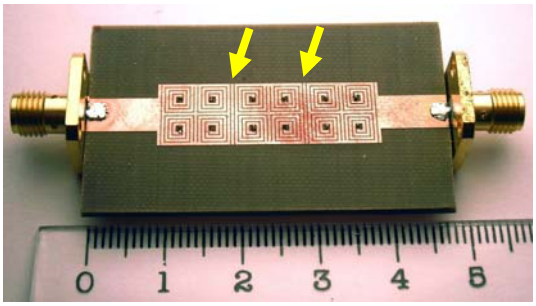

(b)

Figure 13 Fabricated LH transmission lines with weakly coupled adjacent ForeSs: (a) *N*=2 unit cells and (b) *N*=3 unit cells

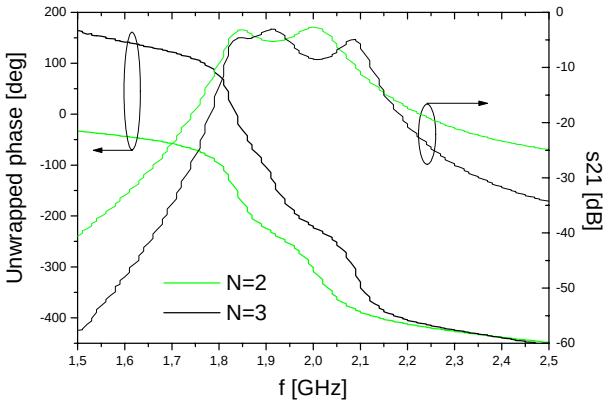

Figure 14 Measured transmission coefficients and unwrapped phase responses of two LH transmission lines with *N*=2 and *N*=3 unit cells

As in the previous case, left-handedness of the proposed structure can be verified by the existence of a phase advance in the pass band. In Figure 14, measured unwrapped phases of transmission coefficients obtained from two lines with N=2 and N=3 unit cells are compared, and backward propagation is demonstrated.

In Figure 15, simulation results for LH lines with different number of the unit cells, N, are shown. It can be seen that the ripple in the pass band is reduced, in comparison to the case of direct coupled unit cells. Again, the steeper response is achieved by using the greater number of the unit cells.

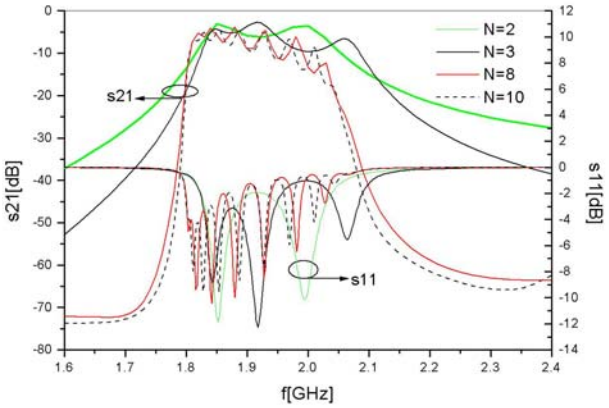

Figure 15 Simulated transmission and reflection coefficients of the proposed LH transmission line with weakly coupled unit cells, for different number of the unit cells, N

To verify the simulation results, LH lines with N=2 and N=3 unit cells were fabricated. The measured responses are shown in Figure 16.

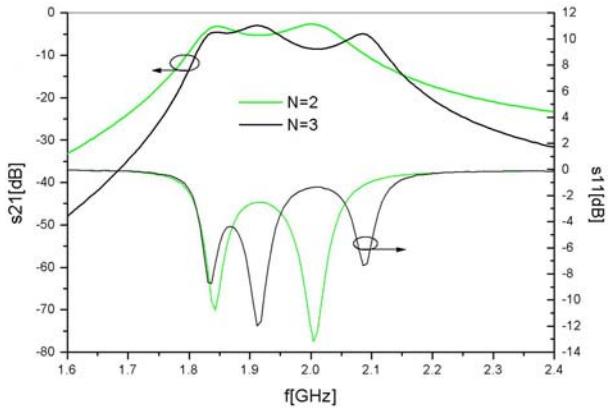

Figure 16 Measured transmission and reflection coefficients of the proposed LH transmission line with weakly coupled unit cells, for *N*=2 and *N*=3 unit cells

A good agreement between the simulated and the measured responses can be observed. By comparing measured responses of two proposed LH transmission line designs, Figure 12 and Figure 16, it can be seen that the vertical lines added between the adjacent unit cells cause a significant reduction of the pass band ripple at the expense of somewhat reduced fractional LH bandwidth, that is in this case approximately equal to 20%.

5. CONCLUSION

A novel super-compact LH unit cell called ForeS is presented. The overall dimensions of ForeS are $\lambda_g/13$ by $\lambda_g/13$, where λ_g denotes the guided wavelength. In contrast to other LH structures, ForeS exhibits low insertion losses and a large design flexibility: by introducing small changes to the inner dimensions of ForeS, resonant frequency tuning range approximately equal to 67% is achieved, i.e. resonant frequency can be varied between 1.038GHz to 3.18GHz. ForeS offers good trade-off between the Q-factor, insertion loss and the dimensions. Furthermore, it exhibits very good out-of-band performance: the second harmonic is positioned at more then four times the first resonant frequency.

ForeS also exhibits great potential for application in electronically reconfigurable circuits: by placing the diodes at the relevant positions and by applying bias voltage, 27% resonant frequency tuning range can be achieved, as well as different in- and out-of-band performances.

By cascading ForeSs, two novel LH transmission lines are designed with different coupling mechanisms between the unit cells. The first type is the LH TL with direct coupling that exhibits fractional LH bandwidth approximately equal to 30%. However, it suffers from high pass band ripple.

The second LH TL design is obtained by inserting vertical lines between the adjacent ForeSs. In this way, coupling between the neighboring unit cells is reduced. This results in somewhat reduced fractional LH bandwidth, equal to 20%, but also in significantly smaller pass band ripple.

ACKNOWLEDGEMENTS

This work is supported by Eureka program (METATEC-METAmaterial–based TEchnology for broadband wireless Communications and RF identification E! 3853 project).

REFERENCES

[1] V. Veselago, "The electrodynamics of substances with simultaneously negative values of ε and μ," *Soviet Physics Uspekhi*, vol. 92, no. 3, pp. 517-526, 1967.

[2] D. R. Smith, W. J. Padilla, D. C. Vier, S. C. Nemat-Nasser and S. Schultz, "Composite medium with simultaneously negative permeability and permittivity," *Phys. Rev. Lett*., vol. 84, no. 18, pp. 4184-4187, May 2000.

[3] A. A. Oliner, "A periodic-structure negative-refractive-index medium without resonant elements," *URSI Dig. IEEE-AP-S USNC/URSI National Radio Science Meeting* 2002, p. 41, 2002.

[4] C. Caloz and T. Itoh, "Application of the transmission line theory of left-handed (LH) materials to the realization of a microstrip LH transmission line," *Proc. IEEE-AP-S USNC/URSI National Radio Science Meeting* 2002, vol. 2, pp. 412–415, 2002.

[5] A. K. Iyer and G. V. Eleftheriades, "Negative refractive index metamaterials supporting 2-D waves," *Proc. IEEE MTT Int. Symp.* 2002, vol. 2, pp. 412–415, 2002.

[6] R. Marqués, J. Martel, F. Mesa, and F. Medina, "Left handed media simulation and transmission of EM waves in sub-wavelength SRR-loaded metallic waveguides", *Phys. Rev. Lett*., vol. 89, pp. 183901-03, 2002.

[7] R. A. Shelby, D. R. Smith, S. C. Nemat-Nasser, and S. Schultz, "Microwave transmission through a two-dimensional, isotropic, left-handed metamaterial," *Appl. Phys. Lett.*, vol. 78, 4, pp. 489, 2001.

[8] G. V. Eleftheriades, A. K. Iyer, and P. C. Kremer, “Planar negative refractive index media using periodically L-C loaded transmission lines,” *IEEE Trans. Microwave Theory Tech.*, vol. 50, pp. 2702-2712, Dec. 2002.

[9] A. Grbic, and G. V. Eleftheriades, "An isotropic three-dimensional negative-refractive-index transmission-line metamaterial," *Journal of Applied Physics,* 98, pp. 043106, 2005.

[10] G. V. Eleftheriades, O. Siddiqui and A.K. Iyer, “Transmission line models for negative refractive index media and associated implementation without excess resonators,’” *IEEE Microwave Wireless Compon. Lett.*, vol. 13, pp. 51-53, Feb. 2003.

[11] C. Caloz, and T. Itoh, ”Transmission line approach of left-handed (LH) materials and microstrip implementation of an artificial LH transmission line,” *IEEE Trans. Ant. and Prop.*, vol. 52, no. 5, pp. 1159-1166, May 2004.

[12] A. Lai, C. Caloz, and T. Itoh, “Composite right/left–handed transmission line metamaterials,” *IEEE Microwave Magazine*, vol. 5, no. 3, pp. 34-50, September 2004.

[13] B. Jokanovic, and V. Crnojevic-Bengin, “Novel reconfigurable left-handed unit cell for filter applications,” *Proc. of PIERS 2007 Conf.*, Bejing, China, March 2007.

LIST OF FIGURE CAPTIONS:

Figure 1 ForeS unit cell with relevant dimensions

Figure 2 Simulated transmission coefficients for four different ForeSs that occupy the same area

Figure 3 (a) Conventional ring resonator and its modifications used for comparison: (b) with horizontal line, (c) with vertical line, (d) with both lines

Figure 4 Simulated transmission coefficients of a conventional ring resonator and its modifications shown in Figure 3

Figure 5 Comparison of simulated transmission coefficients for ForeS_1 with different number of spiral turns, N_s

Figure 6 ForeS unit cell with positions at which diodes can be placed, indicated with light patches

Figure 7 Different configurations obtained by means of electronic reconfigurability: (a) original ForeS (End-Connected Cross), (b) End-Opened Cross, (c) Center-Connected Cross, (d) Center-Disconnected Cross

Figure 8 Measured transmission coefficients of different configurations obtained by means of electronic reconfigurability

Figure 9 Fabricated LH transmission lines with direct coupling of adjacent ForeSs: (a) N=2 unit cells and (b) N=3 unit cells

Figure 10 Measured transmission coefficients and unwrapped phase responses of two LH transmission lines with N=2 and N=3 unit cells

Figure 11 Simulated transmission and reflection coefficients of the proposed LH transmission line with the direct coupling, for different number of the unit cells, N

Figure 12 Measured transmission and reflection coefficients of the proposed LH transmission line with the direct coupling, for different number of the unit cells, N

Figure 13 Fabricated LH transmission lines with weakly coupled adjacent ForeSs: (a) N=2 unit cells and (b) N=3 unit cells

Figure 14 Measured transmission coefficients and unwrapped phase responses of two LH transmission lines with N=2 and N=3 unit cells

Figure 15 Simulated transmission and reflection coefficients of the proposed LH transmission line with weakly coupled unit cells, for different number of the unit cells, N

Figure 16 Measured transmission and reflection coefficients of the proposed LH transmission line with weakly coupled unit cells, for N=2 and N=3 unit cells

LIST OF TABLE CAPTIONS:

TABLE 1 Simulation results for four different ForeSs that occupy the same area

TABLE 2 Simulation results for ForeS_1 with different number of spiral turns, N_s

TABLE 3 Simulation results for ForeS and its modifications